

Prospects for observation of double parton scattering with four–muon final states at LHCb

C.H. KOM^{a,b}, A. KULESZA^c AND W.J. STIRLING^a

^a *Cavendish Laboratory, University of Cambridge, CB3 0HE, UK*

^b *Department of Applied Mathematics and Theoretical Physics, University of Cambridge, CB3 0WA, UK*

^c *Institute for Theoretical Particle Physics and Cosmology, RWTH Aachen University, D-52056 Aachen, Germany*

Abstract

We study the prospects for observing double parton scattering through four–muon final states, forming two opposite–sign muon pairs, in the LHCb experiment in pp collisions at 14 TeV centre of mass energy. We consider two special cases, namely double Drell–Yan and J/ψ –pair production. The kinematic properties and prospects for observing these processes are discussed. We find that the production rate depends strongly on the origin of the four muons, while many kinematic properties can be used to help identify the presence of double parton scattering events.

1 Introduction

The subject of multiple parton interactions has been enjoying a renewed interest over the last few years, driven by the need to understand the full spectrum of hadronic activity at the LHC. The large collision energy available at the LHC increases the probability of scattering of more than just one parton from each hadron. In particular, multiple scattering events with final state particles carrying relatively high transverse momentum should occur much more commonly than at the previously operating hadron colliders. Such observations provide valuable information on the structure of the proton and the parton–parton correlations within. Indeed, processes involving two hard scatterings in one hadron–hadron collision, the so–called double parton scattering (DPS),

have been studied in the 4-jet and the γ +3-jet channels by the AFS [1], UA2 [2], CDF [3] and D0 [4] experiments, and the presence of DPS is now well established.

In order to measure double parton scattering, one needs to consider processes for which the single parton scattering (SPS) background is low or possesses characteristics that allow for the signal to be extracted. To date, phenomenological studies have focused on observation of DPS in hadronic processes such as four jets [5–13], $b\bar{b}$ pairs [14, 15], $b\bar{b}$ pair and two jets [10], Higgs and a gauge boson [16, 17], production of either photons [18, 19], W [20–22] or Z bosons [22] in association with jets, or purely lepton events such as double Drell–Yan [23, 24] and same-sign W -pair production [15, 22, 25, 26].

In the environment of hadronic collisions, purely leptonic signatures offer a clean probe of the underlying scattering mechanisms. A generic property of DPS processes is that they are expected to peak strongly in the low transverse momentum (p_T), low Q^2 phase space region, which is difficult to access with a typical central detector. In final states involving jets, tagging and identifying low p_T jets associated with the DPS signal process is challenging due to the overwhelming QCD background. However multi-lepton, especially muon, final states are much cleaner, making triggering on multi lepton final states with low p_T possible. In this paper we take advantage of the excellent low p_T muon acceptance of the LHCb detector, which can go down to ~ 1 GeV, and focus on four-muon final states that form two opposite-sign (OS) muon pairs in this particular experiment. This should maximize the number of DPS events observed.

Depending on the analysis cuts, in particular on the invariant mass of the OS muon pairs, the DPS signal could be dominated by double Drell–Yan (DDY) production or production of a quarkonium (e.g. J/ψ or Υ) pair, which then decay into four leptons. The possibility of observing DPS in pair-production of quarkonia has been recently investigated in [27–29]. In particular, in Ref. [27] we have argued that the recent measurement of double J/ψ production by the LHCb experiment [30] could already indicate a significant contribution from DPS.

While the production of double J/ψ pairs benefits from a large cross section, the subprocess of DDY, i.e. *single* DY production, is theoretically well understood. For this reason, double Drell–Yan production might be considered a standard-candle DPS process and merits a more detailed investigation. Moreover, the partons involved in these processes are different. DPS double J/ψ production is expected to be dominantly produced by four gluons, whereas for DDY, the initial states at leading order (LO) are two quark–anti-quark pairs. Hence the correlations being probed are different. In this paper, we shall primarily focus on the prospect for observing DPS through the DDY channel. We also comment on some characteristic differences between double J/ψ and DDY production.

The paper is structured as follows. In Section 2 we discuss the DPS signal and SPS background to DDY production at the LHC. Our method of performing calculations and cuts chosen to select the signal appropriate to the LHCb experiment are presented

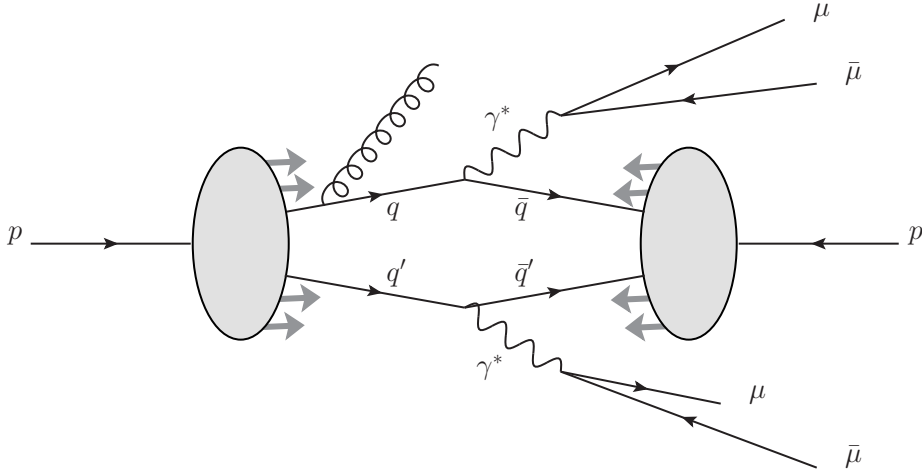


Figure 1: Example Feynman diagram for the DPS double Drell–Yan process.

in Section 3, where we also give the total rates for the processes of interest. In Section 4 we address the differential distributions for the signal and background to the DDY process, followed by a discussion of differences between the DDY and double J/ψ distributions in Section 5, before concluding in Section 6.

2 Double Drell–Yan at LHCb

2.1 DPS signal

The DPS signal process leading to the two OS muon pair final state is assumed to come from two independent hard scatterings of the DY type. An example Feynman diagram is shown in Fig. 1. If we further assume that the longitudinal and the transverse components of the generalized double parton distribution functions can be factorised, and that there are no longitudinal momentum correlations between the partons in the same hadron, the DPS DDY cross section factorizes into a product of two SPS *single* DY cross sections. More precisely, the differential DPS cross section $d\sigma_{\text{DPS}}^{\text{DDY}}$ is written as

$$d\sigma_{\text{DPS}}^{\text{DDY}} = \frac{d\sigma_{\text{SPS}}^{\text{DY}} d\sigma_{\text{SPS}}^{\text{DY}}}{2\sigma_{\text{eff}}}, \quad (1)$$

where

$$d\sigma_{\text{SPS}}^{\text{DY}} = \sum_{a,b} f_a(x_a, \mu_F) f_b(x_b, \mu_F) d\hat{\sigma}_{\text{SPS}}^{\text{DY}} dx_a dx_b, \quad (2)$$

and

$$d\hat{\sigma}_{\text{SPS}}^{\text{DY}} = \sum_{a,b} \frac{1}{2\hat{s}} \overline{|M_{ab \rightarrow \gamma^* \rightarrow l+l^-+X}|^2} d\text{PS}_{l+l^-+X} \quad (3)$$

correspond to the hadronic and partonic single DY process respectively. In the above expressions, \hat{s} is the partonic centre-of-mass energy squared, f_i and x_i ($i = a, b$) are the parton distribution functions (PDFs) and longitudinal momentum fraction for parton with flavour i , and μ_F is the factorization scale. The single DY matrix element and phase space element are denoted by M and $d\text{PS}$ respectively. The factor σ_{eff} captures all the information on the transverse structure of the proton. It is likely to be process and energy dependent, and is the main quantity that a DPS experiment will aim to extract. However, for concreteness, we shall use $\sigma_{\text{eff}} = 14.5$ mb, a value measured in the $\gamma+3$ -jet study by the CDF experiment [3].¹

Recently, questions have been raised [31, 32] about to what extent this intuitive picture can be derived in perturbative QCD. In particular, the assumption of factorization between the longitudinal and transverse components of double parton distributions appears not to be strictly consistent with QCD. It leads to an appearance of the spurious “single-feed” term in the evolution equation for double parton distributions, describing correlations in longitudinal momentum fractions x_i . However, in the current analysis we consider final states produced through DPS with relatively low invariant masses, meaning the incoming partons have on average low longitudinal momentum. Since at low x the parton-parton correlations are expected to be negligible, using single parton distributions $f_i(x_i, \mu_F)$ is likely to be a good approximation.

2.2 SPS background

Example Feynman diagrams for the SPS production process of two OS muon pairs are shown in Fig. 2. They can be classified into two groups: the “double resonance”-type diagrams (Fig. 2a), where both virtual photons are attached to the initial state quarks, and the “single resonance”-type diagrams (Fig. 2b), where the quarks fuse into a γ^* before decaying into four muons via an additional γ^* . In our analysis we consider contributions from both types of diagrams, as opposed to a previous study [24] in which only the first type of diagrams is included.²

2.3 Selection of the DPS signal

As mentioned in the Introduction, in order to observe the DPS signal, the SPS background has to be low, at least in some region of the phase space. In the case of two OS muon pair final states, there is no particular reason why *a priori* the SPS production

¹ A similar value, 15.1 mb, was obtained by the corresponding D0 experiment[4].

²From (electromagnetic) charge consideration, it can be seen that these two types of diagrams are separately gauge invariant. In this sense they could be considered independently.

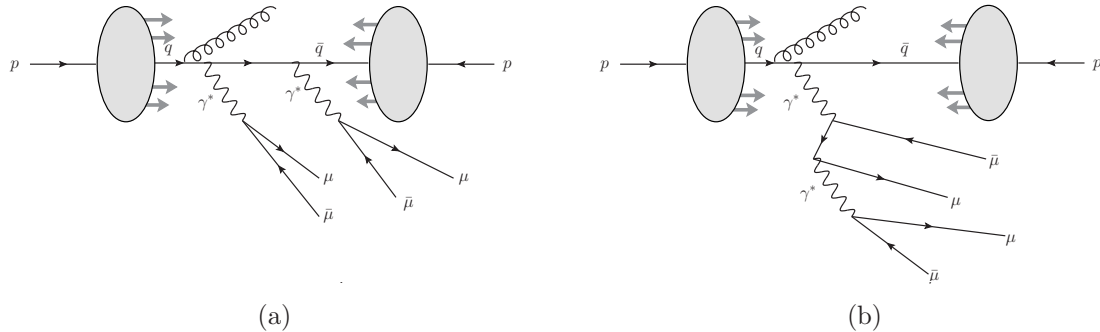


Figure 2: Example Feynman diagrams for the SPS double Drell–Yan process. (a) “double resonance”–type diagrams, where both virtual photons are attached to the initial state quarks, and (b) “single resonance”–type diagrams, where only one virtual photon is attached to the quark line.

rates should be suppressed, as opposed to, e.g., the same–sign W –pair production, where due to electromagnetic charge conservation the SPS process can only occur at higher order in powers of (gauge) couplings than in DPS. Therefore in studying the final state with two OS muon pairs, it is important to exploit different kinematical properties of the SPS and DPS final states.

For the DPS signal, given our independent hard scattering assumption, each of the two OS muon pairs originating from the two γ^* will exhibit p_T balancing at the parton level. The presence of initial state radiation (ISR) will provide a non-zero p_T to each of the γ^* . The independent scattering hypothesis then implies that the azimuthal angular separation between the two γ^* s should be uniformly distributed. On the contrary, for the SPS background, at the parton level the transverse momentum is generally only balanced among all four muons. An implication is that for the two combinatoric ways to form two OS muon pairs, which we shall also call γ^* , both will lead to a configuration in which the two γ^* s travel back–to–back in the transverse plane. However again this picture will be distorted in the presence of ISR. These basic kinematic differences form the basis for identifying the presence of DPS events in previous experimental studies. A number of “pair wise balancing” variables, designed to exploit the different transverse plane behaviour for the DPS and SPS processes, have been introduced in the literature. We shall see that the impact of significant QCD radiation on the low invariant masses being considered will lead to significant deviation from the intuitive parton–level picture, making the usage of such pair wise balancing variables less effective in discriminating DPS from SPS events. On the other hand, “longitudinal” variables are generally less sensitive to these effects. The absolute rapidity difference between two reconstructed J/ψ s was first proposed in [27] as a method to extract DPS from SPS events. We shall see whether a similar strategy

can be used for DDY by constructing a similar variable for the γ^* s.

Another complication is that for DDY there is a two-fold (combinatoric) ambiguity in grouping the four muons into two OS pairs. This ambiguity is absent for double J/ψ , since the “correct” pairing must have $\mu^+\mu^-$ invariant masses lying within a mass window close to the physical J/ψ mass. This leads to a different set of cuts that must be applied to the DDY, which will result in different kinematical distributions. We shall discuss the impact of these effects in more detail in the following sections.

So far, we have considered the irreducible SPS background only. In the low mass region, semi-leptonic decay of heavy quarks and hadron mis-identification can fake the signal, and are important sources of background. These backgrounds have been studied in LHCb in the context of single DY [33], and it was found that a multi-variate selection strategy based on the isolated nature of the muons produced in DY processes can be used to achieve purities of 95% down to $m_{\mu^+\mu^-} = 2.5$ GeV. A similar method could presumably be used for DDY, however a detailed study is beyond the scope of the present study.

3 Event simulation

We now discuss how the DPS signal and SPS background events are generated. The predictions for the DPS signal are obtained using the multi-parton scattering model in `Herwig++ v2.4.2` [34], which allows for generation of two hard scatterings in every event. We use the following (default `Herwig++`) $\alpha(Q^2)$ definition: $\alpha(Q^2) = \alpha(0)/(1 - K(Q^2))$, where $\alpha(0) = 1/137.04$, and $K(Q^2) = \frac{\alpha(0)}{3\pi}(13.4955 + 3\log(Q^2/\text{GeV}^2)) + 0.00165 + 0.00299\log(1.0 + Q^2/\text{GeV}^2)$. We use `MSTW 08 NLO PDFs` [35], and set the factorization scale μ_F for both 2-to-2 single DY subprocesses at $\mu_F = \sqrt{\hat{s}}$, which can be different for the two subprocesses in the same event. `Herwig++` enables us to take higher order QCD effects into account in the parton shower. In principle `Herwig++` can also include effects of intrinsic p_T -smearing of incoming partons. However currently p_T -smearing is applied only to the “primary” hard process. In order to provide intrinsic p_T -smearings for *both* hard subprocesses, we switch off the default intrinsic Gaussian p_T functionality during event generation, and implement independent p_T smearings to the two hard subprocesses using the same Gaussian model. For illustration, the root-mean-square intrinsic p_T in this model, σ , is set to a conservative value of 2 GeV.

The SPS events with two OS muon pairs are generated using the package `MADGRAPH v5.1.2.4` [36]. Here the same $\alpha(Q^2)$ definition as in the DPS process is used. We include both “double resonance” and “single resonance”-type diagrams, as discussed in Section 2. In the low invariant mass region being considered in this analysis, it is sufficient to consider only the Feynman diagrams with two γ^* , i.e. no diagrams with (virtual) Z -bosons are included. For consistency, in the experimental analysis, the contributions from processes involving Z 's have to be eliminated. This can be

achieved by imposing an upper cut on the invariant mass of the four muons, $m_{4\mu}$. Such a cut is also useful in enhancing the signal-to-background (S/B) ratio, as the DPS signal is expected to have comparatively low four-muon invariant mass. The factorization scale is set at $\mu_F = \sqrt{\hat{s}}$, i.e. $m_{4\mu}$. The parton level events generated by MADGRAPH are interfaced to Herwig++ for parton showering. As in the DPS process, the MSTW 08 NLO PDFs are used and an intrinsic Gaussian p_T smearing is applied after event generation, with the parameter σ set to 2 GeV.

We now discuss event selection. For the muons to be observed in the LHCb detector, the pseudorapidity (η) and p_T of each muon has to obey:

- $1.9 < \eta < 4.9$,
- $p_T > 1$ GeV.

Apart from the muons coming from the decay of γ^* , the simulated events can also contain additional muons generated by the decay of hadrons formed in the hadronisation process. To be conservative, we select events with exactly four muons passing the above acceptance cuts, and that they form two OS muon pairs. Additionally, we request that the events correspond to processes with γ^* decaying into muon pairs by avoiding the low mass hadronic resonance and the Z resonance regions with the following cuts:

- $m_{\mu^+\mu^-} > 4$ GeV for *all* four $\mu^+\mu^-$ combinations,
- $m_{4\mu} < 40$ GeV.

Note that the cut $m_{\mu^+\mu^-} > 4$ GeV must apply to all $\mu^+\mu^-$ combinations, instead of only two of them. This is because there are potentially dangerous backgrounds involving low mass hadronic resonances, for example J/ψ . These resonances could lead to high invariant masses from *mismatched* $\mu^+\mu^-$ pairs, i.e. pairs that do not come from the decay of the same resonance. A cut on all $\mu^+\mu^-$ pairs will however also apply to the *true* pairing, which of course has a low $\mu^+\mu^-$ invariant mass, and reject the event as a result.

Furthermore, contributions from $\Upsilon(1S)$ and its higher resonances $\Upsilon(2S)$ and $\Upsilon(3S)$, when combined with other source of muons, can lead to two OS muon pairs. The Υ background can be suppressed by rejecting events with

- 9.2 GeV $< m_{\mu^+\mu^-} < 10.5$ GeV for *any* of the four $\mu^+\mu^-$ combinations,

where the mass window is obtained from the recently published result by LHCb on Υ production [37].

We will refer to the cuts above as the set of “basic cuts” for the DDY analysis. We assume 100% detection efficiency for an event passing the above cuts. The cross sections for the production of four-muon final states in pp collisions at 7 and 14 TeV, after applying basic cuts, are displayed in Table 1.

DDY cross sections [fb] at LHCb		
	DPS	SPS
7 TeV	0.08	0.43
14 TeV	0.16	0.68

Table 1: DPS and SPS DDY cross sections (in fb) for pp collisions at 7 and 14 TeV. For clarity, only the results with parton shower and intrinsic Gaussian p_T broadening $\sigma = 2$ GeV are shown.

double J/ψ cross sections [pb] at LHCb		
	DPS	SPS
7 TeV	3.16	1.70
14 TeV	7.69	2.62

Table 2: DPS and SPS double J/ψ cross sections (in pb), including the branching ratio $\mathcal{BR}(J/\psi \rightarrow \mu^+\mu^-)$. For clarity, only the results with parton shower and intrinsic p_T broadening $\sigma = 2$ GeV are shown.

For comparison, we also present predictions for four-muon final states originating from a decay of a J/ψ -pair, produced in pp collisions at 7 and 14 TeV. Our line of analysis follows the one of [27], where we studied the double J/ψ production at LHCb for a collision energy of 7 TeV, i.e. we apply the same methods of calculations and the same parameter values as in [27]. As for the DDY analysis, the set of single muon cut is given by:

- $1.9 < \eta < 4.9$,
- $p_T > 1$ GeV.

The narrower range $2 < \eta < 4.5$ in the analysis of [27] was motivated by the cuts used by the LHCb collaboration in the first experimental analysis of double J/ψ production [30]. Out of the two combinatoric ways to form two OS pairs, the combination with the two invariant masses closest to the physical J/ψ masses is chosen. This requirement is sufficient to discriminate between the combinations, as the OS muon pairs originate from J/ψ resonances. In our event simulation, we do not include effects due to finite detector resolution. As for the DDY analysis, MSTW 08 NLO PDFs are used and 100% reconstruction and detection efficiency is assumed. The DPS and SPS cross sections obtained after basic cuts and the invariant-mass selection criterion are applied are displayed in Table 2.

At present, it is not yet understood how to systematically include higher order effects within the DPS framework. The inclusion of the parton shower in our simulations may be considered as a possible first step towards predictions with higher order corrections taken into account. However, the shower evolution does not change the total

event rate of the parton level, if integrated over the full phase space. Therefore it is illustrative to consider the size of the next-to-leading (NLO) K -factors for the total cross sections.

In the context of our calculations, the appropriate K -factor would be defined by the ratio of the total cross section at NLO calculated using NLO pdfs to the LO total cross section using NLO pdfs. For the $pp \rightarrow \gamma^* \gamma^* \rightarrow e^+ e^- \mu^+ \mu^-$ process at 14 TeV, calculations with the MCFM package [38] give, for the set of basic cuts considered here, $K_{\text{NLO}} = 1.7$.

For comparison, the K -factor for *single* DY, defined in the same way as above, is $K_{\text{NLO}} = 3.0$, when the cross sections are calculated with invariant mass $m_{\mu^+ \mu^-}$ between 4 and 40 GeV. This could indicate an enhanced S/B ratio if higher order effects were taken into account.

Based on the DPS and SPS rates quoted in Tables 1 and 2, we see that the measurement of DPS in four-muon final states will be more challenging for the DDY process, when compared to double J/ψ production. In particular, the rates for DPS DDY are of $\mathcal{O}(0.1)$ fb and $\mathcal{O}(0.2)$ fb at the 7 and 14 TeV LHC respectively, with relatively low S/B ratios. However possible improvements could be made. For example, it might be possible to better understand the Υ background by investigating the behaviour of the inclusive Υ sample [37] that contains an extra pair of muons when the “basic cuts” are applied.

We also recall that in our calculation we assume a fixed value for $\sigma_{\text{eff}} = 14.5$ mb. This value might be process and scale dependent, and as discussed in Section 2 is a parameter to be determined by experiment. Therefore in the next section we will focus on studying kinematical distributions and investigate if further kinematical cuts can be introduced to improve the S/B ratio, as well as facilitating the extraction of σ_{eff} . With luminosity of a few inverse femtobarn, the number of DDY events expected at the 7 TeV LHC is likely to be too low. For this reason only results for the 14 TeV LHC will be presented.

4 Kinematic distributions for the DDY process

In this section we study differential cross sections for the production of four-muon final states originating from a decay of two γ^* after the set of basic cuts has been applied. To see the effects of parton showering and intrinsic p_T smearing, we present three sets of predictions for the SPS and DPS production mechanism:

- Parton level only (labelled as “PL” in the plots),
- Parton level + parton shower (labelled “PS”),
- Parton level + parton shower + intrinsic p_T smearing (labelled “PS+ σ ”).

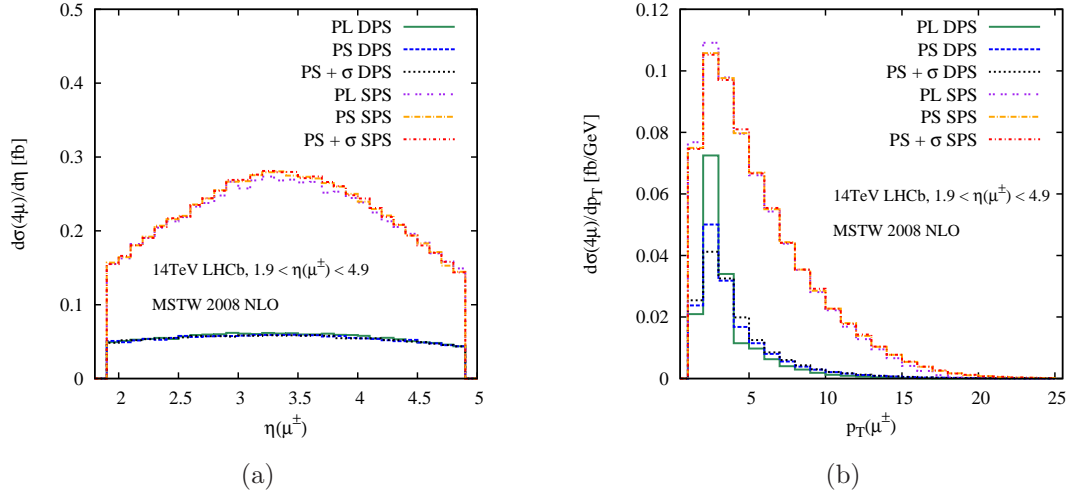


Figure 3: The DPS and SPS single μ distributions in (a) η and (b) p_T for the process $pp \rightarrow \gamma^* \gamma^* \rightarrow \mu^+ \mu^- \mu^+ \mu^-$ at the LHC with 14 TeV.

The rapidity and transverse momentum distributions for a single μ are shown in Fig. 3. We see that in the entire η and p_T range considered here, the SPS background dominates over the DPS signal. The η distribution for the SPS background is more central within the allowed η range. This is because the four muons originate from a single hard process, and it is more likely for all of them to be within the η acceptance if the four-muon system falls in the centre of this allowed region. The p_T distributions of SPS and DPS muons peak at about the same value, with the SPS distribution being slightly harder. Apart from the DPS p_T distribution, we see that the other distributions shown in Fig. 3 are not sensitive to ISR or intrinsic p_T .

Next we study the separation of DPS and SPS events using their different kinematic behaviour in the transverse plane. As discussed in Section 2, at parton level, provided that the $\mu^+ \mu^-$ pairs are grouped correctly, the vector p_T sum of the two OS pairs in a DPS event will be balanced *separately*, i.e. $\mathbf{p}_T = 0$. For the SPS, such p_T balancing is generally achieved only among all 4 muons, which implies that the \mathbf{p}_T of the two $\mu^+ \mu^-$ pairs will be opposite to each other, resulting in a back-to-back configuration in the transverse plane. These differences can in principle be used to distinguish the DPS from the SPS process. In addition, these can be used to find the $\mu^+ \mu^-$ pairing that corresponds to the actual DPS process, and allow further analysis based on the kinematic properties of these pairs, i.e. the γ^* in our present context.

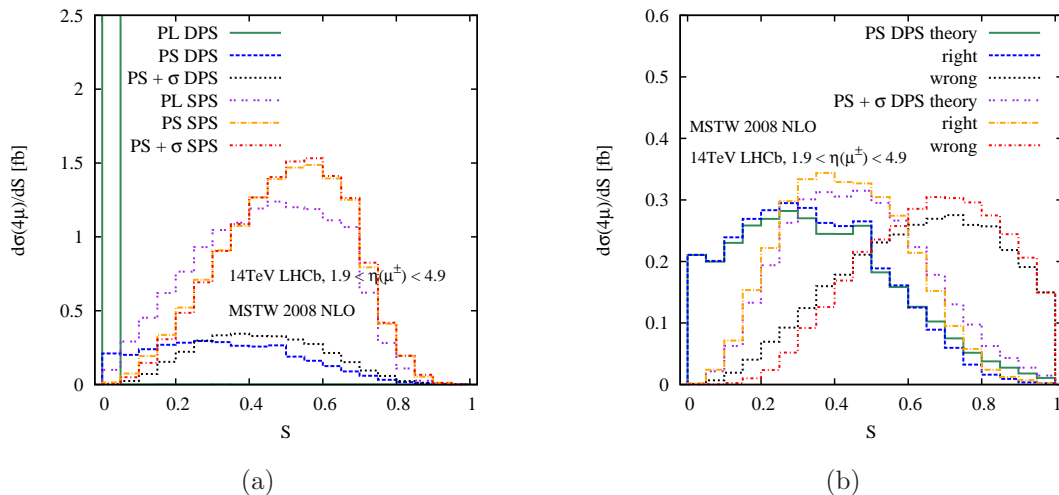


Figure 4: (a) The DPS and SPS differential distributions in the p_T -balance variable S for the $\mu^+\mu^-$ combination that minimises S , and (b) comparison of the DPS differential distributions for the “right”, obtained by minimizing S , and “wrong” $\mu^+\mu^-$ pairs with the theoretical distribution obtained by always pairing a $\mu^+\mu^-$ pair from the same γ^* together. In plot (b), the top (bottom) three keys correspond to parton shower simulations without (including) intrinsic p_T smearing.

To select one of the two combinatoric ways to form two OS muon pairs, we select the combination that minimises the following pair-wise balancing variable (S):

$$S \equiv \frac{1}{2} \left(\frac{|\mathbf{p}_{T\mu_1^+} + \mathbf{p}_{T\mu_1^-}|}{p_{T\mu_1^+} + p_{T\mu_1^-}} + \frac{|\mathbf{p}_{T\mu_2^+} + \mathbf{p}_{T\mu_2^-}|}{p_{T\mu_2^+} + p_{T\mu_2^-}} \right), \quad 0 < S < 1 \quad (4)$$

For the DPS signal, at parton level the correct pairing always leads to $S = 0$, while ISR and intrinsic p_T effects will distort the picture. Other variables similar to S have been defined in the literature, for e.g. those in Ref. [4]. We have checked that their performance are similar to the S variable defined in Eq. 4

The S distributions are displayed in Fig. 4. As we can see, the DPS parton level result is in strict contrast to the SPS process. In fact, from Fig. 4a it can be seen that the values of S close to 0.5–0.7 are the most preferred for SPS, whereas S peaks sharply in the lowest bin for the DPS at parton level, as expected. Unfortunately, radiation and intrinsic p_T effects change the picture dramatically. While the S distribution for the SPS process gets modified in a relatively moderate way, the additional gluon radiation in the DPS process spoils the p_T balance to a large extent, flattening and spreading the distribution up to high values of S . This, of course, significantly decreases the power of the variable S to discriminate between the SPS and DPS mech-

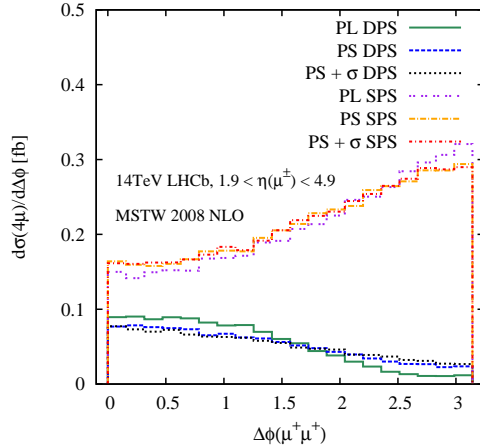


Figure 5: The DPS and SPS differential distributions in the angle $\Delta\phi$ between the two μ^+ for the process $pp \rightarrow \gamma^*\gamma^* \rightarrow \mu^+\mu^-\mu^+\mu^-$ at the LHC with 14 TeV.

anisms. In Fig. 4b we compare the S distributions between the pairings obtained in the above procedure (“right”), the other pairing (“wrong”) and the theoretical distribution (“theory”) obtained by insisting that the $\mu^+\mu^-$ pair comes from the same γ^* . We see that the “theory” and “right” distributions are broadly similar, indicating the effectiveness of the minimum S criterion to pair the OS muons coming from decay of the same γ^* in DPS, despite the presence of radiation and intrinsic p_T effects. We estimate that using this requirement leads to selecting the correct $\mu^+\mu^-$ pair for around 75% of the DPS event sample. For the SPS background, due to much more complicated kinematical features, the minimum S criterion does not select any particular physical SPS configurations.

We next study the distribution in the angle on the transverse plane between the two same-sign muons, $\Delta\phi$, here chosen to be $\mu^+\mu^+$, *cf.* Fig. 5. The SPS events tend to occur with bigger angular separation, which can be traced back to the tendency for the $\mu^+\mu^-$ pairs to be back-to-back in the transverse plane at parton level. For the DPS signal, one would expect that independent scatterings lead a flat $\Delta\phi$ distribution. However, the requirement that all four $\mu^+\mu^-$ pairs pass the invariant mass cut preferentially selects events with all OS μ^- -pairs apart, resulting in a smaller angular separation for same-sign muons. The effect for the opposite-sign muons can be observed in Fig. 6, which shows the angular distributions for the “right” and “wrong” combinations of $\mu^+\mu^-$ pairs. The “right” pairs minimize S , making it more likely for DDY that the two paired muons come from decay of the same γ^* . In particular, at LO where the DY γ^* have no p_T , choosing S to be minimal tends to pick out only those $\mu^+\mu^-$ combinations which are back-to-back, see Fig. 6a. The preference towards larger angular separation

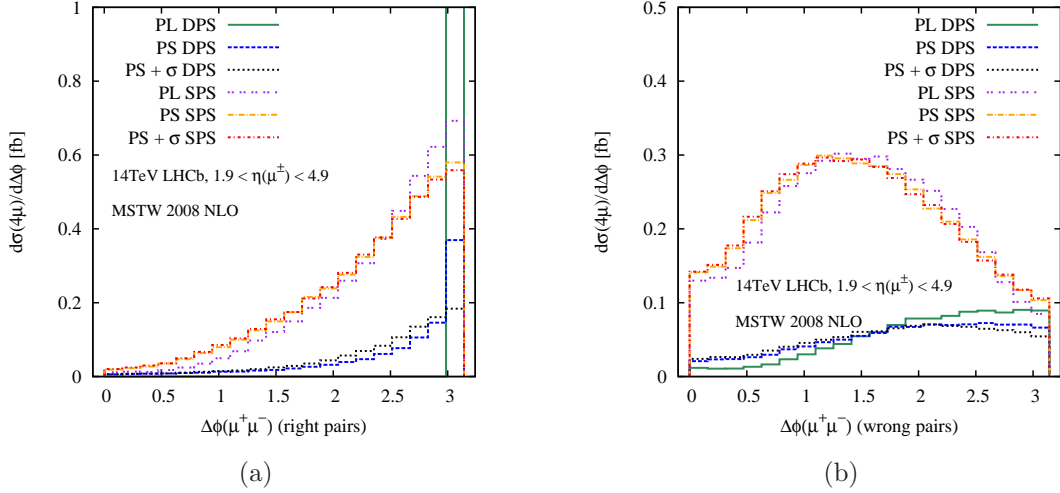


Figure 6: The DPS and SPS differential distributions in the angle $\Delta\phi$ between the opposite-sign muons for the (a) “right” and (b) “wrong” pairs for the process $pp \rightarrow \gamma^*\gamma^* \rightarrow \mu^+\mu^-\mu^+\mu^-$ at the LHC with 14 TeV.

between “right” DPS pairs remains after including radiation and smearing effects. However, the SPS events also tend to have larger angular distributions between the OS muons in pairs that minimize the value of S . This tendency is no longer true for SPS “wrong” $\mu^+\mu^-$ pairs, i.e. the combination with a larger value of S . In fact, the qualitative effect is opposite to that of $\mu^+\mu^+$ shown in Fig. 5, which is not unexpected since both distributions involve azimuthal angular separations between muons from the wrong pairs, and would be correlated to certain extent.

Further differential distributions involving $\mu^+\mu^-$ pairs, selected using the S -variable criterion, are shown in Figs. 7 (p_T and rapidity y) and 8 ($\Delta\phi$ and Δy). As expected, the p_T distribution of the DPS muon-pairs is peaked at very low values, lower than those for the SPS distribution, even after the showering and smearing effects are included, *cf.* Fig. 7a. In particular, in the low p_T region an excess of events compared to a pure SPS model prediction might be observed. As shown in Fig. 7b, both the SPS and DPS have fairly symmetric rapidity distributions for the constructed $\mu^+\mu^-$ pairs, with very similar distributions. In Fig. 8a we present the distributions for the angle (in the transverse plane) between the $\mu^+\mu^-$ pairs from the “right” combination, $\Delta\phi(\mu^+\mu^-, \mu^+\mu^-)$. The DPS distribution is relatively uniform over the whole range of $\Delta\phi(\mu^+\mu^-, \mu^+\mu^-)$, consistent with the assumption of two independent scatterings in the DDY process. The SPS contribution, on the other hand, peaks at $\Delta\phi(\mu^+\mu^-, \mu^+\mu^-) = \pi$, which is a consequence of the transverse momentum conservation for the SPS process at leading order, as already discussed. Fig. 8b shows the properties of the SPS and DPS processes

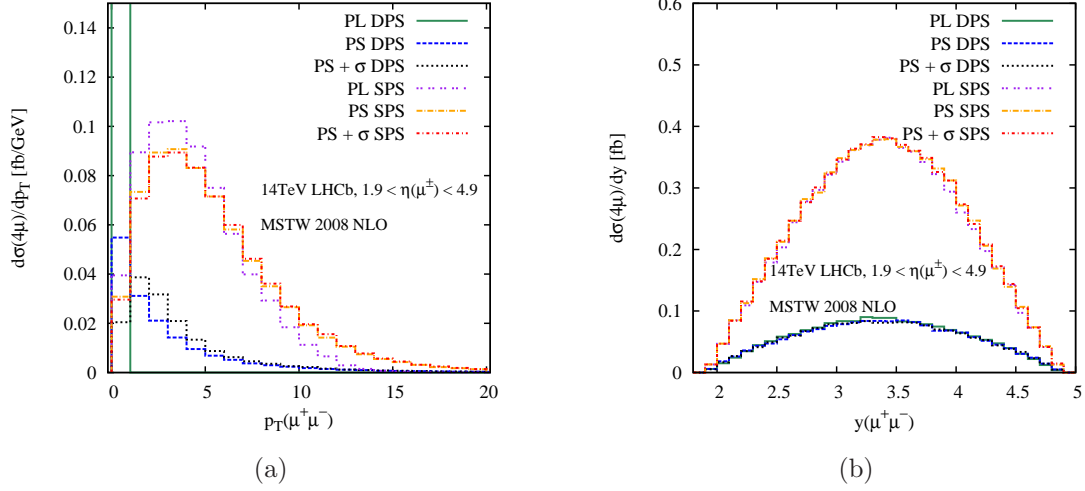


Figure 7: The DPS and SPS differential distributions in (a) p_T and (b) y for the “right” $\mu^+\mu^-$ pairs for the process $pp \rightarrow \gamma^*\gamma^* \rightarrow \mu^+\mu^-\mu^+\mu^-$ at the LHC with 14 TeV.

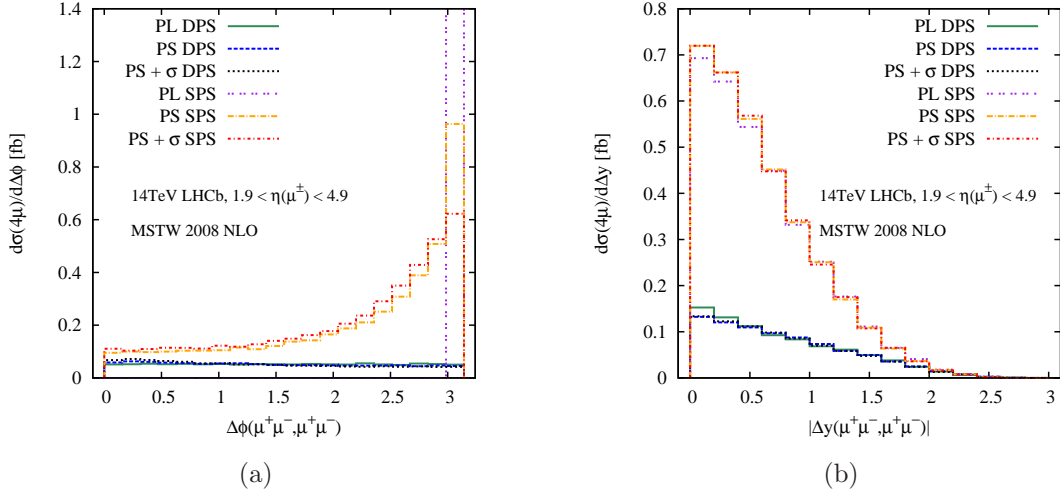


Figure 8: The DPS and SPS differential distributions in (a) the angle $\Delta\phi$ between the two $\mu^+\mu^-$ pairs and (b) the absolute value of the difference in rapidity $|\Delta y|$ for the “right” muon-pairs for the process $pp \rightarrow \gamma^*\gamma^* \rightarrow \mu^+\mu^-\mu^+\mu^-$ at the LHC with 14 TeV.

with respect to correlations in the longitudinal direction, or more precisely the absolute value of the difference between the rapidities of the two $\mu^+\mu^-$ pairs, $|\Delta y(\mu^+\mu^-, \mu^+\mu^-)|$. As opposed to distributions depending on variables measured in the transverse plane,

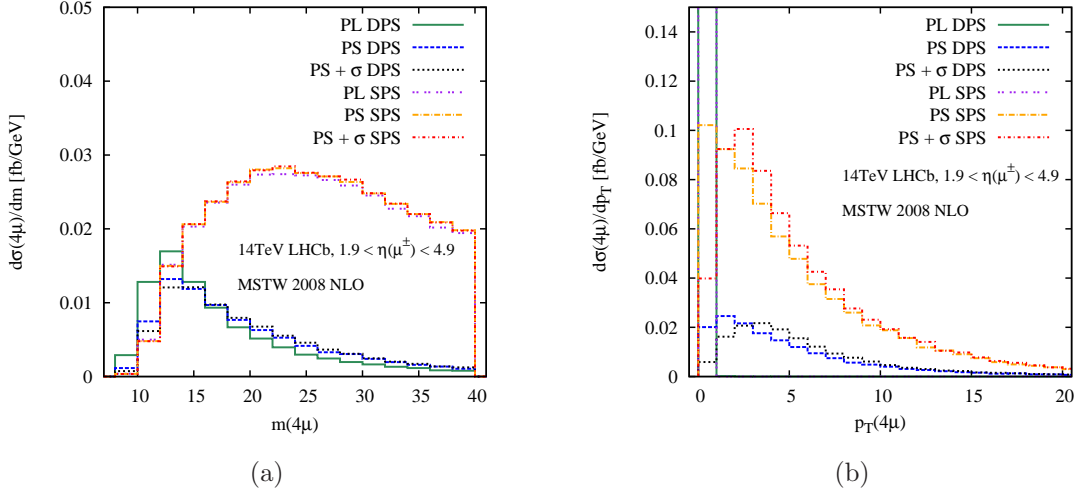


Figure 9: The DPS and SPS differential distributions for all four muons in (a) the invariant mass $m(4\mu)$ and (b) the transverse momentum $p_T(4\mu)$ for the process $pp \rightarrow \gamma^*\gamma^* \rightarrow \mu^+\mu^-\mu^+\mu^-$ at the LHC with 14 TeV.

distributions involving rapidity variables exhibit very little dependence on radiation and intrinsic smearing, an effect first noticed and put to use in [27]. We see that as $|\Delta y|$ increases, the SPS contribution falls more steeply than that of DPS, although the difference is not as strong as in the double J/ψ analysis in [27].

Yet another possibility for studying the DPS and SPS distributions is offered by the distributions sensitive to quantities constructed from four vectors of all muons in the final state. In Fig. 9 we investigate the invariant mass $m(4\mu)$ and the transverse momentum $p_T(4\mu)$ distributions of all four muons. A significant difference in the invariant mass distribution can be observed for the SPS and DPS mechanisms, *cf.* Fig. 9a, and an excess of DPS events might be observed in the low $m(4\mu)$ region. This can be traced back to the lower cut on the $\mu^+\mu^-$ invariant mass, which, as already noted, favours configurations with all OS μ -pairs apart. For DPS the impact of the cut is relatively mild, as the independent scattering hypothesis implies that OS pairs from different hard scatterings tend to be well separated. This is not the case for the SPS background, which results in higher invariant mass of all leptons in the final state. From this figure, it can be inferred that events with $m(4\mu) > 40$ GeV are dominated by the SPS background, and hence could form a control region for the SPS background estimation. A more aggressive cut on $\max m(4\mu)$, down to around 30 GeV, appears to be possible. Such a cut would reduce the SPS background by around 30%, while having a relatively mild impact on the signal. However, we remain conservative here and refrain from doing so. The $p_T(4\mu)$ distribution shown in Fig. 9b measures the

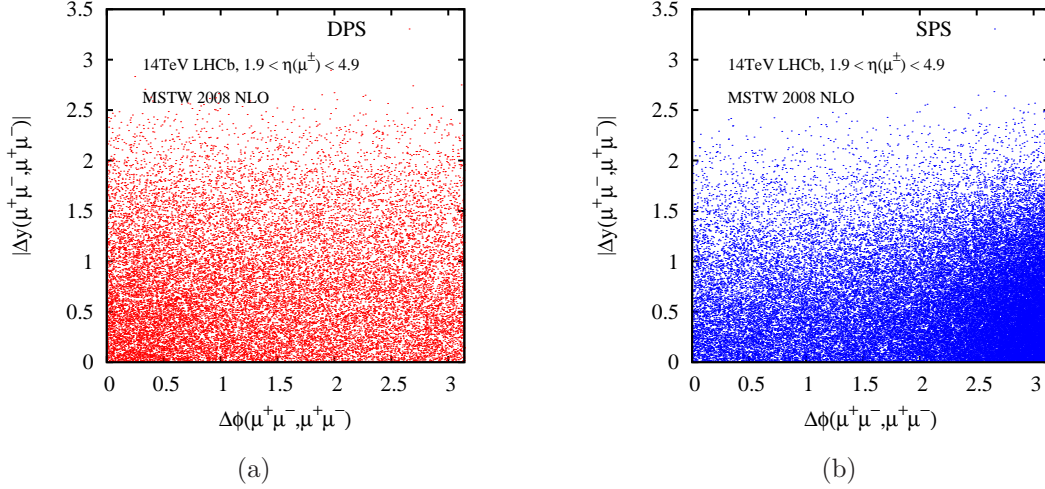


Figure 10: Scatter plots on the $(\Delta\phi(\mu^+\mu^-, \mu^+\mu^-), |\Delta y(\mu^+\mu^-, \mu^+\mu^-)|)$ plane for the (a) DPS and (b) SPS mechanism for the process $pp \rightarrow \gamma^*\gamma^* \rightarrow \mu^+\mu^-\mu^+\mu^-$ at the LHC with 14 TeV.

sensitivity of the SPS and DPS to extra radiation, simulated by parton showering, and intrinsic smearing. Both distributions are affected by these effects in a similar way, with the peak of the showered distribution at approximately the same value and moving to higher p_T as the smearing is switched on.

Since the two types of correlations, i.e. in the transverse plane and in the longitudinal directions, between the muons in the final state probe different kind of information on the same process, it is interesting to study the double differential distributions in $\Delta\phi(\mu^+\mu^-, \mu^+\mu^-)$ and $|\Delta y(\mu^+\mu^-, \mu^+\mu^-)|$. In Fig. 10 we present scatter plots in the $\Delta\phi(\mu^+\mu^-, \mu^+\mu^-)$ and $|\Delta y(\mu^+\mu^-, \mu^+\mu^-)|$ plane for the DPS and SPS samples. The former appears to be slightly more populated in the region with small $\Delta\phi$ and $|\Delta y|$, whereas events of the latter tend to occupy the corner of large $\Delta\phi(\mu^+\mu^-, \mu^+\mu^-)$ and small $|\Delta y(\mu^+\mu^-, \mu^+\mu^-)|$.

Concluding, observing DPS through four-muon final states from DDY scatterings seems to be a challenging task due to its low production rate, *cf.* Table 1. Although an excess of DPS events could be observed in the low $p_T(\mu^+\mu^-)$ and $m(4\mu)$ regions, the studied differential distributions between the SPS and DPS event samples do not show kinematical differences that are striking enough to justify putting additional hard cuts (perhaps with the exception of $m(4\mu)$) at the cost of further reducing the signal yield.

On the other hand, we see that in addition to $p_T(\mu^+\mu^-)$ and $m(4\mu)$, variables such as S , $\Delta\phi(\mu^+\mu^-, \mu^+\mu^-)$, $|\Delta y(\mu^+\mu^-, \mu^+\mu^-)|$ or $\Delta\phi(\mu^+\mu^-)$ of the wrong muon-pairs also show moderate, non-trivial differences between the DPS and SPS components, and we

are able to understand the origin of their different distributions. To fully utilize these differences, it would be more effective to apply the template method, as is done for example in the $\gamma + 3j$ studies in CDF and D0 to extract the DPS fraction. Moreover, we see from the double differential distribution in Fig. 10 that additional information can be obtained by simultaneously considering more than one kinematic quantity.

5 Kinematic distributions for double J/ψ production

As seen in Section 3, after applying sets of basic cuts the total cross sections for double J/ψ production at LHCb are significantly higher than the equivalent cross sections for the DDY process. Even more importantly the S/B ratio is also better. This makes double J/ψ production an excellent candidate process to observe DPS [27–29].

Methods to study double J/ψ and to extract the DPS signal from the SPS background have been discussed in some detail in [27]. Here we extend this study by comparing the different properties between double J/ψ and DDY in pp collisions at 14 TeV.

There are a few important differences between double J/ψ and DDY. First, their production is initiated by different partons: while double J/ψ production is driven by the gluon–gluon fusion process, both SPS DDY and the single DY subprocess in DPS DDY require, at lowest order, a quark and an antiquark. The longitudinal momentum densities of these partons are different, which would lead to different rapidity distributions for the $\mu^+\mu^-$ pairs. Different initial–state partons also affect the parton shower, and hence p_T . However, the hard scales of the double J/ψ and DDY are also different, which will in turn affect the amount of QCD radiation. The combined effect has an impact on p_T as well as azimuthal angular separations in the transverse plane of the reconstructed objects.³

In Fig. 11 we show the rapidity and $\Delta\phi(\mu^+\mu^-, \mu^+\mu^-)$ distributions of the $\mu^+\mu^-$ pairs from double J/ψ production. Here the invariant mass of a $\mu^+\mu^-$ pair readily determines if they originate from a J/ψ resonance or not, and hence there is no ambiguity in pairing up the OS muons. Compared with DDY (*cf.* Fig. 7b), we see in Fig. 11a that both the double J/ψ SPS and DPS are more central, with the effect of SPS stronger. This is due to the smaller gluon densities at high parton x compared to the light (anti) quarks, making high η values for the $\mu^+\mu^-$ pairs less likely. In Fig. 11b the impact of QCD radiation on $\Delta\phi(\mu^+\mu^-, \mu^+\mu^-)$ is clearly seen, where the distribution including parton shower peaks slightly towards zero, instead of π , the parton level result. This should be compared with the corresponding figure for DDY, Fig. 8a, which shows a milder radiation effect.

³In the present study we do not attempt to disentangle the effects on p_T from these sources.

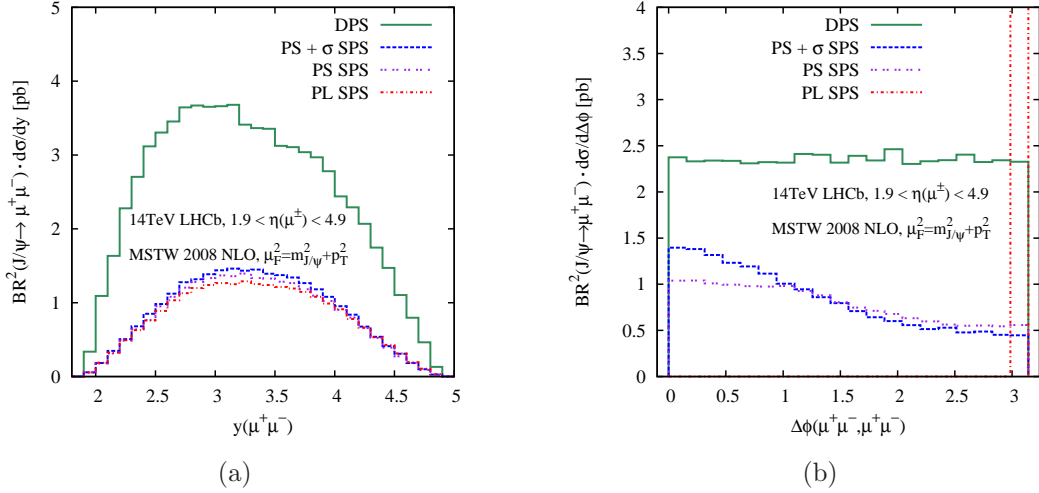


Figure 11: The DPS and SPS differential distributions in (a) y and (b) $\Delta\phi(\mu^+\mu^-, \mu^+\mu^-)$ of $\mu^+\mu^-$ pairs for the process $pp \rightarrow J/\psi J/\psi \rightarrow \mu^+\mu^-\mu^+\mu^-$ at the LHC with 14 TeV.

A consequence of the well defined way to pair up the OS muons is that it is not necessary to introduce the variable S as a way to group the muons, although it could still be used to help distinguish the SPS and DPS components. Since for the SPS DDY process the pairing according to value of S does not correspond to finding two μ 's from a decay of the same γ^* , more significant differences between DDY and double J/ψ are expected for the SPS background.

The four-muon invariant mass distribution for double J/ψ production is shown in Fig. 12a. The DPS component peaks at higher value of $m(4\mu)$ than the SPS component. The reverse is observed for DDY, *cf.* Fig. 9a. This can partly be attributed to the $\mu^+\mu^-$ invariant mass cut applied in the DDY analysis, which will tend to push the SPS $m(4\mu)$ distribution towards higher values. Of course there is no equivalent mass cut in the J/ψ study, since there is no ambiguity in pairing up the muons. A quantity related to $m(4\mu)$ is $|\Delta y(\mu^+\mu^-, \mu^+\mu^-)|$, as in the centre of mass frame, a larger $m(4\mu)$ will imply a larger $|\Delta y(\mu^+\mu^-, \mu^+\mu^-)|$ given a fixed $p_T(\mu^+\mu^-)$. This distribution is displayed in Fig. 12b. The observation for double J/ψ of a more steeply falling $|\Delta y|$ for the SPS is consistent with the more steeply falling $m(4\mu)$. For DDY, the broader SPS $m(4\mu)$ distribution implies that $|\Delta y|$ would be more slowly falling, thus making $|\Delta y|$ less effective as a variable to extract DPS from SPS component in DDY.

Finally, we note that overall our current studies reinforce the statements made in [27] regarding the importance of radiation and intrinsic p_T smearing effects for the observables involving quantities measured in the transverse plane. At the same time, we confirm the relative insensitivity to these effects on the variables measuring correlations

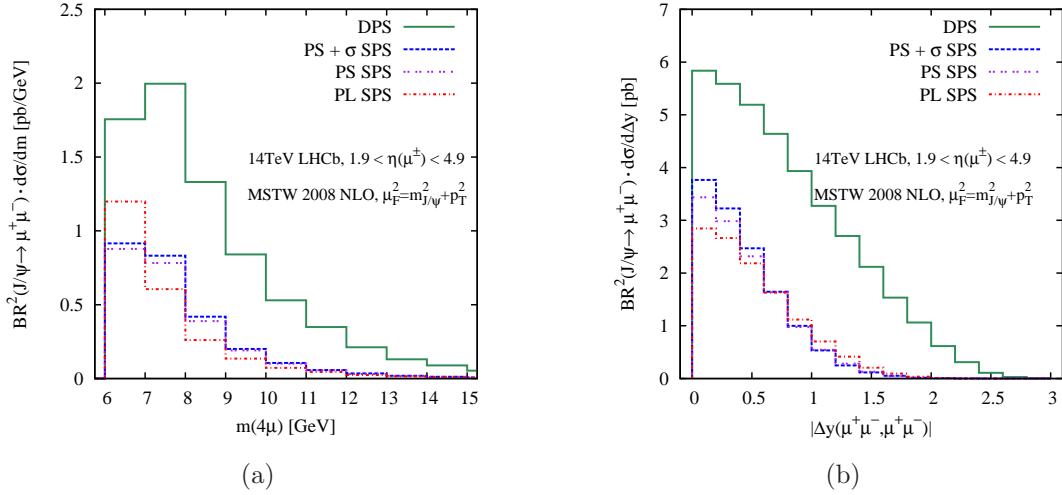


Figure 12: The DPS and SPS differential distributions for (a) the invariant mass $m(4\mu)$ and (b) the absolute value of the difference in rapidity $|\Delta y(\mu^+\mu^-, \mu^+\mu^-)|$ for the $\mu^+\mu^-$ pairs for the process $pp \rightarrow J/\psi J/\psi \rightarrow \mu^+\mu^-\mu^+\mu^-$ at the LHC with 14 TeV.

in the longitudinal direction. Therefore it could be beneficial to investigate in more detail how “longitudinal variables” may be used to facilitate other DPS searches in the future.

6 Conclusions and outlook

Measurements undertaken at the LHC will be crucial for improving the theoretical description of multiple parton scattering. In this paper we have studied the production of two OS muon pairs via two hard scatterings of the DY type. DY production is considered a standard candle process at hadron colliders. The leptonic final states provide very clean experimental signatures, while the status of theoretical predictions is under control. All this makes the production of two OS muon-pairs a model candidate process for probing the nature of DPS.

Depending on the invariant mass of the OS muon pairs, they may originate either from continuum (γ^*) or a hadronic resonance, e.g. J/ψ . In the course of our study, we have found that at 7 TeV, the DDY cross section and luminosity are too low for this process to be observed with the LHCb detector. The prospects for observing DDY should improve at 14 TeV LHC given the increases in cross section, S/B ratio and luminosity. On the other hand, the production of the same final state through a double J/ψ process possesses characteristics which should allow a measurement of DPS at the LHCb in pp collisions at both 7 and 14 TeV. However, we stress that these two

processes are sensitive to different initial state partons ((anti)quark–(anti)quark for DDY and gluon–gluon for double J/ψ). Hence they probe different correlation effects and provide complementary input to double parton distributions.

For the same reason, it might prove valuable to additionally investigate four muon final states where one muon pair comes from a decay of γ^* while the second originates from the decay of a low–mass resonance, e.g. J/ψ . The cross section for such a process might be expected to lie between double J/ψ and DDY, and hence is likely to be observable. Furthermore, although in this paper we have concentrated on pairs of J/ψ 's as resonant sources of four–muon final states at low invariant masses, another promising opportunity to study DPS can be offered by studying higher mass resonances, in particular involving Υ production. For example, measurement of σ_{eff} for both double J/ψ and double Υ processes could provide information on the scale dependence of the two–gluon parton distribution function. This would complement well the study of scale dependence that could be performed in e.g. $\gamma + 3j$, $W^\pm W^\pm$ and other jet–based signatures proposed for the general purpose detectors ATLAS and CMS [39].

Upon completion of this paper, a suggestion to study double Υ has been put forward in [29].

Acknowledgements

This work has been supported in part by the Helmholtz Alliance “Physics at the Terascale”, the Isaac Newton Trust and the STFC. AK would like to thank the High Energy Physics Group at the Cavendish Laboratory for hospitality. CHK thanks the Institute for Theoretical Particle Physics and Cosmology at RWTH Aachen University and the Particle and Astroparticle Physics group at MPIK Heidelberg for hospitality while part of the work was carried out.

References

- [1] T. Akesson *et al.* [Axial Field Spectrometer Collaboration], *Z. Phys.* **C34**, 163 (1987).
- [2] J. Alitti *et al.* [UA2 Collaboration], *Phys. Lett.* **B268**, 145-154 (1991).
- [3] F. Abe *et al.* [CDF Collaboration], *Phys. Rev.* **D47**, 4857-4871 (1993). *Phys. Rev. Lett.* **79**, 584-589 (1997). *Phys. Rev.* **D56**, 3811-3832 (1997).
- [4] V. M. Abazov *et al.* [D0 Collaboration], *Phys. Rev.* **D81**, 052012 (2010).
- [5] N. Paver and D. Treleani, *Nuovo Cim. A* **70** (1982) 215; *Phys. Lett.* **B146** (1984) 252.

- [6] B. Humpert, Phys. Lett. **B131** (1983) 461.
- [7] B. Humpert and R. Odorico, Phys. Lett. B **154** (1985) 211.
- [8] L. Ametller, N. Paver and D. Treleani, Phys. Lett. B **169** (1986) 289.
- [9] M. L. Mangano, Z. Phys. C **42** (1989) 331.
- [10] E. L. Berger, C. B. Jackson, G. Shaughnessy, Phys. Rev. **D81** (2010) 014014. [arXiv:0911.5348 [hep-ph]].
- [11] S. Domdey, H. -J. Pirner, U. A. Wiedemann, Eur. Phys. J. **C65** (2010) 153-162. [arXiv:0906.4335 [hep-ph]].
- [12] B. Blok, Yu. Dokshitzer, L. Frankfurt, M. Strikman, Phys. Rev. **D83** (2011) 071501. [arXiv:1009.2714 [hep-ph]].
- [13] B. Blok, Yu. Dokshitzer, L. Frankfurt, M. Strikman, [arXiv:1106.5533 [hep-ph]].
- [14] A. Del Fabbro, D. Treleani, Phys. Rev. **D66** (2002) 074012. [hep-ph/0207311].
- [15] E. Cattaruzza, A. Del Fabbro, D. Treleani, Phys. Rev. **D72** (2005) 034022. [hep-ph/0507052].
- [16] A. Del Fabbro, D. Treleani, Phys. Rev. **D61** (2000) 077502. [hep-ph/9911358].
- [17] M. Y. Hussein, Nucl. Phys. Proc. Suppl. **174** (2007) 55 [arXiv:hep-ph/0610207]; arXiv:0710.0203 [hep-ph].
- [18] M. Drees and T. Han, Phys. Rev. Lett. **77** (1996) 4142 [arXiv:hep-ph/9605430].
- [19] O. J. P. Eboli, F. Halzen, J. K. Mizukoshi, Phys. Rev. **D57** (1998) 1730-1734. [hep-ph/9710443].
- [20] R. M. Godbole, S. Gupta and J. Lindfors, Z. Phys. C **47** (1990) 69.
- [21] E. Maina, JHEP **0904** (2009) 098 [arXiv:0904.2682 [hep-ph]].
- [22] E. Maina, JHEP **0909** (2009) 081 [arXiv:0909.1586 [hep-ph]].
- [23] C. Goebel, F. Halzen and D. M. Scott, Phys. Rev. D **22** (1980) 2789.
- [24] F. Halzen, P. Hoyer, W. J. Stirling, Phys. Lett. **B188** (1987) 375-378.
- [25] A. Kulesza and W. J. Stirling, Phys. Lett. B **475** (2000) 168 [arXiv:hep-ph/9912232].

- [26] J. R. Gaunt, C. H. Kom, A. Kulesza and W. J. Stirling, *Eur. Phys. J. C* **69** (2010) 53 [arXiv:1003.3953 [hep-ph]].
- [27] C. H. Kom, A. Kulesza, W. J. Stirling, *Phys. Rev. Lett.* **107** (2011) 082002 [arXiv:1105.4186 [hep-ph]].
- [28] S. P. Baranov, A. M. Snigirev, N. P. Zotov, [arXiv:1105.6276 [hep-ph]].
- [29] A. Novoselov, [arXiv:1106.2184 [hep-ph]].
- [30] LHCb Collaboration, LHCb-CONF-2011-009.
- [31] M. Diehl, A. Schafer, *Phys. Lett.* **B698** (2011) 389-402. [arXiv:1102.3081 [hep-ph]].
- [32] J. R. Gaunt, W. J. Stirling, [arXiv:1103.1888 [hep-ph]].
- [33] LHCb Collaboration, LHCb-CONF-2009-014.
- [34] M. Bahr, S. Gieseke, M. A. Gigg, D. Grellscheid, K. Hamilton, O. Latunde-Dada, S. Platzer, P. Richardson *et al.*, *Eur. Phys. J.* **C58**, 639-707 (2008).
- [35] A. D. Martin, W. J. Stirling, R. S. Thorne and G. Watt, *Eur. Phys. J. C* **63** (2009) 189 [arXiv:0901.0002 [hep-ph]].
- [36] J. Alwall, M. Herquet, F. Maltoni, O. Mattelaer, T. Stelzer, [arXiv:1106.0522 [hep-ph]]; J. Alwall, P. Demin, S. de Visscher, R. Frederix, M. Herquet, F. Maltoni, T. Plehn, D. L. Rainwater *et al.*, *JHEP* **0709**, 028 (2007). [arXiv:0706.2334 [hep-ph]]; F. Maltoni, T. Stelzer, *JHEP* **0302**, 027 (2003). [hep-ph/0208156].
- [37] LHCb Collaboration, LHCb-CONF-2011-016.
- [38] J. M. Campbell, R. K. Ellis, *Phys. Rev.* **D60** (1999) 113006. [hep-ph/9905386], and <http://mcfm.fnal.gov/>
- [39] MPI@LHC 2010: 2nd International Workshop on Multiple Partonic Interactions at the LHC, Glasgow, 29 Nov– 3 Dec 2010. <http://www.mpi2010.physics.gla.ac.uk/Home.html>